ECS Transactions, 3 (6) 205-215 (2006)
10.1149/1.2357071, copyright The Electrochemical Society

Rough Surface Adhesion Mechanisms for Wafer Bonding.

F. Rieutord[a], L. Capello[a], R. Beneyton[b], C. Morales[b], A.-M. Charvet[b], H.Moriceau[b]

[a] CEA-DRFMC, 17 rue des Martyrs F-38054 GRENOBLE Cedex 9 FRANCE
[b] CEA-DRT/LETI-DIHS-LTFC, 17 rue des Martyrs F-38054 GRENOBLE Cedex 9 FRANCE

Wafer bonding can be viewed as an example of rough surface adhesion. We show that formalisms developed to describe rough surface adhesion can be rescaled to nanometer range and applied to silicon wafer bonding, with results that fit well with experimental observations.

Introduction

The interaction between two solid surfaces is a subject of considerable interest that has been studied since dates starting centuries ago (da Vinci, Amontons, Coulomb). More recently, the problem of understanding the contact mechanics laws (e.g. friction/load laws) on a microscopic scale led to the development of models associated to the statistical description of surfaces (1). These models are mainly adapted to common surfaces i.e. machined surfaces with roughness in the micrometer range. The transposition of such models to the scale of silicon roughness, in the nanometer range, is the purpose of the present paper.

Although silicon surfaces are among the flattest surfaces available, we will show that silicon wafer bonding is a textbook example of the interaction between two rough surfaces. If we consider for the sake of simplicity the case of a so-called hydrophobic bonding, the equilibrium situation can simply be described as that of two rough surfaces attracted to each other by Van der Waals forces, finally balanced by hard wall contact forces.

Roughness description of silicon

The description of the statistics of silicon roughness has been the subject of several studies. Typically, for standard wafers, the roughness measured depends on the lengthscale considered. For standard microelectronics preparations of silicon, all wavelengths are present in the roughness spectrum, with a 1D power spectral density

that decays as a Lorentzian at short (i.e. below 1μm) wavelengths (2). Here we will be interested in these high frequencies mainly, because very long wavelengths can be accommodated by deformation of the substrate, with a little price to pay in elastic energy. We shall assume that the two silicon surfaces can be described by random rough surfaces with a Gaussian vertical distribution of roughness.

This can be checked using e.g AFM or X-ray scattering. The AFM image of a wafer having received a standard chemical surface treatment is shown Fig.1(left). Different statistical parameters can be extracted from the image, among which the height distribution profile which is shown Fig1 (right).

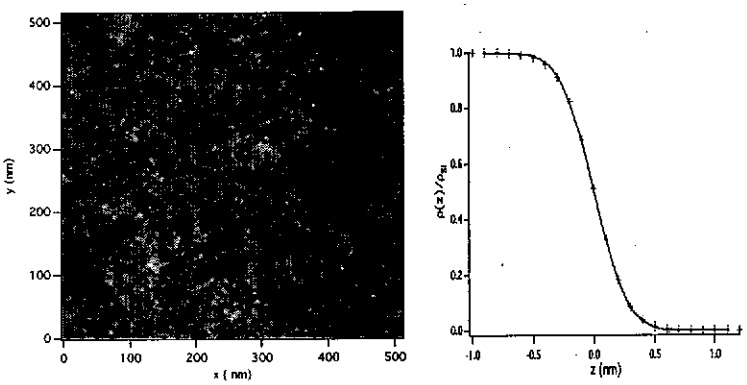

Figure 1. Left: AFM image of a silicon surface 0.5x0.5 μm^2. The height scale is 2nm black to white. Right: Integrated height (roughness) distribution from the image, the solid line is a fit using a Gaussian model (error function) of width 0.22nm.

In addition, parameters related to in-plane spatial variations can be extracted from the image, that will be used to model rough surface interactions:

-Number of summits per unit area N_0. This parameter can be estimated from various techniques including line profile analysis, image processing with thresholding and particle analysis. A typical value of N_0=0.02 nm^{-2} is found.

-Average distribution of summit heights: it is similar to the roughness amplitude and is found to be σ=0.2nm in our example.

-Radius of curvature of the asperities R. A typical value of R=10nm is found. We believe these values and especially N and R should be taken as order of magnitude only, as the experimental resolution of the measurement technique may influence the result. It should be noted that these three quantities are not independent from each other. It has been shown that for random surfaces, their product should be constant. In our case the product $N_0R\sigma$ is 0.04 which is in the correct predicted range.

Interaction between two rough surfaces

The problem of two interacting rough surfaces is equivalent to the interaction between a rigid flat plane and a single elastic rough surface provided that the parameters of the rough surface (Elastic modulus E and roughness σ) are renormalized.

$$\sigma^* = \sqrt{\sigma_1^2 + \sigma_2^2}$$
$$\frac{1}{E^*} = \frac{1}{E_1} + \frac{1}{E_2}$$

Such a process allows one to calculate the number of summits in contact, the actual area in contact and the force due to the compression of the asperities as a function of the (renormalized) separation distance d/σ^*.

Assuming a Gaussian distribution of summit asperities with elastic Hertzian compression of the highest ones, Greenwood and Williamson (1) found the following expressions for the number of summits in contact N, the surface area A and the bearing force P

$$N = N_0 F_0(d/\sigma^*)$$
$$A = A_0 (N_0 R\sigma^*)\pi F_1(d/\sigma^*) \quad [1]$$
$$P = N_0 R^{1/2}\sigma^{*3/2}\ 4/3E^* F_{3/2}(d/\sigma^*)$$

where E* and σ* are effective Young modulus and roughness distribution:

$$E^* = \frac{E}{2(1-\nu^2)} \text{ and } \sigma^{*2} = 2\sigma^2.$$

The functions $F_n(d)$ derive from the Gaussian statistics weight function. They read:

$$F_n(d) = \frac{1}{\sqrt{2\pi}} \int_d^\infty (z-d)^n \exp(-\frac{z^2}{2}) dz \quad [2]$$

Let us note that in our description, we first assume no adherence exists at contact spots. This is justified when no chemical bonds establish between the contact areas which is the case for low temperature bondings.

Expressions [1] derive from the Hertz model for the compression of a single spherical asperity: the relations between the area A and force P and the displacement (penetration) δ read: $A=\pi R\delta$ and $P=4/3E\ R^{1/2}\delta^{3/2}$, hence the exponents n in [1] and [2].

As an example, the force curve corresponding to expression [1] with silicon surface parameters is represented as the dashed line in figure 2.

Attractive forces between the two surfaces

The attractive forces between two silicon wafers can be in a first approximation restricted to Van der Waals forces. Their expression then reads

$$F = \frac{H}{6\pi d^3}$$

where d is the distance between the two surfaces and H the Hamaker constant. Of course in the case of rough surfaces that come in contact this distance may vary greatly, from 0 at contact points to values larger than d between asperities. We will assume however that these variations are smeared out, considering that this description is obtained as a result of integration of pair interactions.

As such, the description probably underestimates the attractive force between the two solids. Interactions around the contact points can be taken into account (Deryaguin), which corresponds to adhesive contact models (see after). The inclusion of such interaction corresponds to the so-called Deryaguin-Müller-Toporov (DMT) model of adhesion (3). The integral of the interactions (potential U(r)) over a single contact can be shown to add an adherence force per contact $F=2\pi\ U(d)\ R$ where R is the radius of curvature of the contact. The adhesion energy is related in this case to the value of the potential at the minimum distance.

In the case of large smooth contacts with large radii of curvature, this approach can be used (4). In our approach, we neglect in a first time the specific interaction occurring close to contact points. This is justified in the room temperature bonding case as we saw that the contacts have very small radii of curvature and we shall see that there are very few contacts.

The Hamaker constant to be taken depends on the material across which the interactions take place. In the case of an hydrophobic bonding, no water is present at the interface and the inner medium is air. Hence we take (5):

$$H=H_{Si/Air/Si}= 21\ 10^{-20}J$$

The attractive force curve is represented as a solid line on figure 2.

Equilibrium: balance of forces

The equilibrium situation is readily obtained by balancing the attractive force to the repulsive contact forces. The equilibrium point is obtained for a distance of 0.9nm typically. This value is large compared to the rms roughness (0.2nm) of the substrate.

Hence a very sma
Gaussian statistics,
of the apparent surf

Concerning the forc
with the separation
force required to
difference between
of bond strength ob
usually underestima

Figure 2. Balance
compression repul
The equilibrium d
point.

It should be noted
case similar quanti
contact surface are
simplicity but ex
effects.

E

X-ray reflectivity
because it has b
millimeter of silic
nanometer level di
The principle of
recall that it allo
interface. In the c
dip in electron de
interested in.

Hence a very small fraction of the asperities are actually in contact. Using the Gaussian statistics, expression [1] predicts that $A/A_0=0.003$, i.e. only a small fraction of the apparent surface do actually contact.

Concerning the forces, one can see that the repulsive part of the force decays quickly with the separation distance, due to the Gaussian statistics of summit heights. The force required to separate the two plates (the bond strength) is the maximum difference between the two curves i.e. typically 5 MPa. This is the order of magnitude of bond strength observed experimentally (6), although direct force measurements are usually underestimating the intrinsic strength, due to defects.

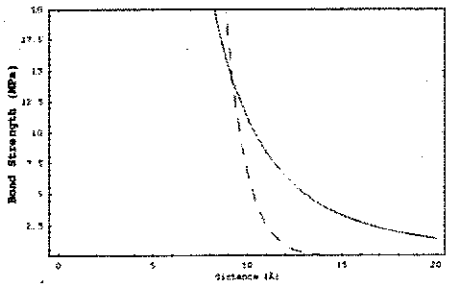

Figure 2. Balance between Van der Waals attraction (solid line) and asperity compression repulsion (dashed line) as calculated using Gaussian roughness models. The equilibrium distance and bond strength can be predicted from the intersection point.

It should be noted that using a plastic model for the asperity compression yield in this case similar quantitative results for the equilibrium distance, the bond strength and the contact surface area. In the following we shall use elastic models only for the sake of simplicity but exact quantitative results would require the inclusion of plasticity effects.

Experimental Tests: X-ray Reflection Experiments

X-ray reflectivity using hard X-rays is a good tool to investigate bonding interface because it has both the penetrating power to reach an interface buried below a millimeter of silicon (typically) while having the resolution and sensitivity to probe nanometer level distances via interferences.

The principle of the method has already been explained in other papers (7). Let us recall that it allows the determination of the electron density profile across an interface. In the case of wafer bonding, the profile will typically have the shape of a dip in electron density, whose width and depth are the two main parameters we are interested in.

In the case of room temperature hydrophobic bonding, the reflection curve is shown fig.3 and the corresponding density profile fig.6 (solid line). The distance between the two surfaces corresponding here to the FWHM of the electron density dip, is readily obtained from the period of the fringe. Note that only one and a half fringes are visible here due a limited accessible intensity range and to the fact that reflectivity decays with incident angle. The data are normalized here to q^4 (where $q=4\pi \sin\theta/\lambda$ is the wavevector transfer), masking this effect. Yet the width of the profile can be measured accurately: w=0.87±0.01nm.

This data is in good agreement with the prediction of figure 2, taking into account the different uncertainties of the parameters describing the rough surface.

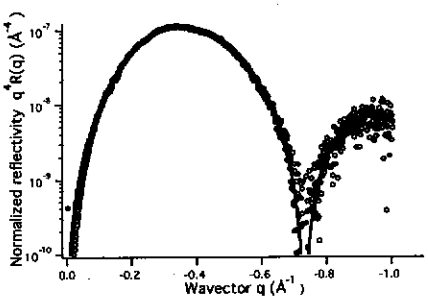

Figure 3. X-ray reflection on a bonding interface. The fringe spacing gives the gap width while the contrast (intensity) gives the closure of the interface

The contrast of the fringes can be used to measure the overlap of the two electron density profiles of the matching surfaces. Here it is found that basically no overlap exist at least to a level that could be detected using X-rays. The density contrast between silicon and the interface zone is equal to the density of silicon , meaning the interface is virtually empty. This is in line with the large distance of equilibrium (0.87nm), compared to the roughness of silicon (0.2nm). Note that this roughness of the two surfaces can be measured in-situ with X-ray also. The roughness is obtained through the damping of the fringes, as a rough surface reflects electromagnetic radiation less than a sharp one. The damping factor can be expressed by $\exp(-q^2\sigma^2)$ where q is the wavevector transfer. Only the very few highest asperities are stiff enough to withstand the load due to Van der Waals forces.

When the system is
adhesive contacts to
the contact level is si
total energy, now inc
Keeping a Hertzian
function of the separ

where w is the adhes
plane and the surfac
der Waals, capillary)

Using expression [1]

where $\theta = \left(\frac{E^* \sigma^{3/2}}{R^{1/2} w}\right)$

surface energies).
Expression [3] is wi
a Bradley-type De
surface parameters a
of 2, corresponding
the two mean sum
adherence is brough
rapidly, as the price
energy gain when u

Another calculation
Johnson, Kendall a
the relations betwee
use the relation
displacement. The

where $P_c=(3\pi/2)wR$

Behaviour upon annealing

When the system is heated, the interface between the two wafers evolves from non-adhesive contacts to adhesive contacts. The approach to be used to include adhesion at the contact level is similar to the previous one. We shall balance force or minimize the total energy, now including a contribution from the contact area.
Keeping a Hertzian model for calculating the elastic energy and the contact area as a function of the separation distance z, we get

$$E_{tot}(z) = \int_z^\infty P(u)du - wA(z)$$

where w is the adhesion energy per unit surface area and z is the distance between the plane and the surface. Here the additional contribution of extra adhesive forces (van der Waals, capillary) are neglected as their contribution to adhesion energy is small.

Using expression [1] for P(z) and A(z), we get

$$\frac{4}{3\pi}\theta = \frac{F_0(z)}{F_{3/2}(z)} \qquad [3]$$

where $\theta = \left(\frac{E^*\sigma^{3/2}}{R^{1/2}w}\right)$ is a so-called adhesion parameter (it is the ratio of elastic to surface energies).
Expression [3] is within a factor of 2 the same as that obtained by Gui et al. (4) using a Bradley-type Deryaguin-Müller-Toporov (DMT) model (3). With the previous surface parameters and taking w=1J/m2, we obtain an adhesion parameter of the order of 2, corresponding to a normalized equilibrium distances z=d/σ close to zero. Hence, the two mean summit heights of the two surfaces lie within the same plane. When adherence is brought into the system, the two surfaces come very close to each other rapidly, as the price to pay in elastic energy remains small compared to the adhesive energy gain when using flat silicon surfaces.

Another calculation can be made within the adhesive contact framework, developed by Johnson, Kendall and Roberts (JKR, (8)). Making the contacts be adhesive changes the relations between interpenetration and pressure or surface area. We can in this case use the relation derived for the JKR model of adhesion between force and displacement. The relation reads

$$P/P_c = g(\delta/\delta_c) \qquad [4]$$

where $P_c=(3\pi/2)wR$ and $\delta_c= (P_c^2/(3K^2R))^{1/3}$ with $K=4/3E^*$.

In the adhesive case, an additional force due to adhesion exists at contact points, changing the relation between the load P and the displacement δ, from a standard $P \propto \delta^{3/2}$ in the Hertz model to expression [4]. The g function is shown Fig.4.

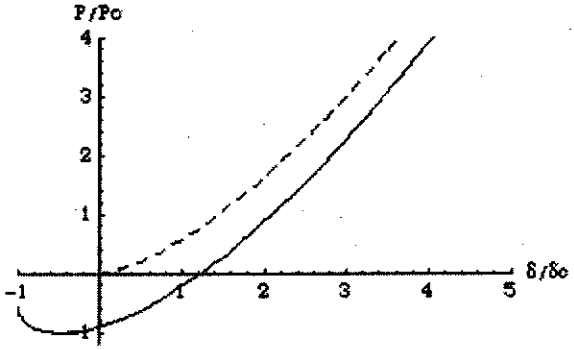

Figure 4. Hertz (non-adhesive) (dashed line) vs JKR (adhesive) (solid line) pressure ↔ displacement relations for individual asperity compression.

The total adhesion force can be obtained integrating the individual forces at contact points (given by g(z)) over the different asperity levels with a Gaussian weight function. Qualitatively, the results are similar to the previous model: as soon as there is an adhesion at the contact points, the mean distance between the two wafers decreases to values comparable to the mean roughness σ and the actual contact area increases significantly, i.e. the interface fills up. The dependence is shown Fig.5.

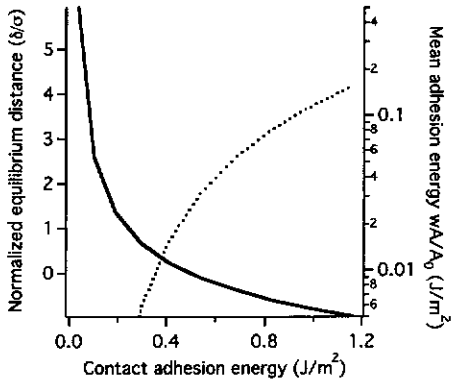

Figure 5. Calculated equilibrium distance in the JKR model as a function of the adhesion energy (solid line, left axis). The resulting apparent bonding energy (i.e. the contact area times the contact bonding energy) is also plotted (dotted line, right axis).

This is what is obse
after annealing neces
as the contact point
i.e. about $4J/m^2$.

When observing wit
the depth of the ele
the interface. In the
around 500°C, a ten

Figure 6. Gap

Note that rough su
independent contact
area fraction A/A_0 i
more difficult to ma

Finally it should be
of the interface an
below (Fig.7). Th
techniques (9) are
shown that the di
preparation lie on
interface closure a
destructive manner
bond velocity meas

This is what is observed experimentally: obtaining a bonding energy of 0.5 to 1 J/m2 after annealing necessarily requires that the contact area be a significant fraction of A_0 as the contact point adhesion energy should not exceed the cohesion energy of silicon i.e. about $4J/m^2$.

When observing with X-rays bonding interfaces that have been annealed, we see that the depth of the electron density deficit decreases, in accordance with a filling up of the interface. In the hydrophobic case for instance (Fig.6), this filling up is observed around 500°C, a temperature above which the adhesion energy increases strongly.

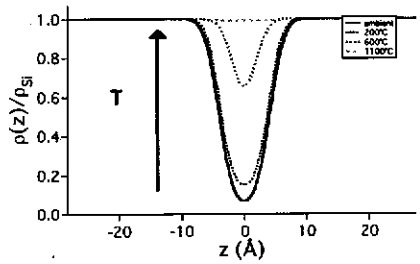

Figure 6. Gap closing of an hydrophobic bond as a function of temperature.

Note that rough surface adhesion models are established under the assumption of independent contacts. Clearly this assumption will no longer be valid when the contact area fraction A/A_0 is large or the distance is small. Hence quantitative predictions are more difficult to make in this case.

Finally it should be mentioned that a direct correlation can be made between the filling of the interface and the adhesion energy. This is illustrated in the figure displayed below (Fig.7). The bonding energies measured using the standard blade opening techniques (9) are plotted versus the interface filling as measured with X-rays. It is shown that the different data points obtained with different annealing or surface preparation lie on the same master curve. Hence the X-ray measurement of the interface closure appears as an attractive technique to measure adherence in a non-destructive manner, complementing other techniques such as blade-opening (9) or bond velocity measurements (10).

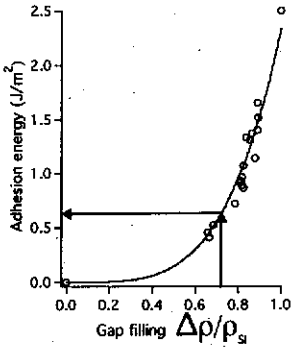

Figure 7. Relation between gap closure as measured by X-ray reflectivity and bonding energy. The data points correspond to samples having received different surface treatments

Conclusion

We have put forward a model for wafer bonding derived from classical random rough surface contact mechanics. The model allows the prediction of key physical parameters such as the mean equilibrium distance between the wafers, real contact area or bond strength. The surface parameters for the model have been obtained from AFM or X-ray measurements. The results have been tested against X-ray interface reflectivity measurements and classical bonding strength or energy measurements with a good agreement.

References

1. J.A. Greenwood, J.B.P. Williamson, *Proc. Roy. Soc.,* **A295,** 300 (1966).
2. E. Marx, I.J. Malik, Y.E. Strausser, T. Bristow, N.Podjue, J.C. Stover, *J. Vac. Sci. Technol. B,* **20,** 31 (2002).
3. B.V. Derjaguin, V.M. Muller, Y.P. Toporov, *J. Colloid. Interf. Sci.,* **53,** 314 (1975).
4. C. Gui, M. Elwenspoek, N. Tas, J.G.E. Gardeniers, *J. Appl. Phys.,* **85,** 7448 (1999).
5. R.H. French, R.M. Cannon, L.K. DeNoyer, Y.-M. Chiang, *Solid State Ionics,* **75,** 13 (1995).
6. D. Resnik, D. Vrtacnik, U. Aljancic, S. Amon, *Sensors and Actuators,* **80,** 68 (2000).
7. F. Rieutord, J. Eymery, F. Fournel, D. Buttard, R. Oeser, O. Plantevin, H. Moriceau, and B. Aspar, *Phys. Rev. B,* **63,** 125408, (2001).
8. K.L. Johnson, K. Kendall, A.D. Roberts, *Proc. Roy. Soc.*, **A324**, 301 (1971).

K.L. Johnson,
9. Q.-Y. Tong, U
10. F. Rieutord, E
(2005).

K.L. Johnson, *Contact Mechanics*, Cambridge University Press (1985).
9. Q.-Y. Tong, U. Gösele, *Semiconductor Wafer Bonding*, Wiley (1999).
10. F. Rieutord, B. Bataillou and H. Moriceau, *Phys. Rev. Lett.*, **94**, 236101, (2005).